



OPEN ACCESS

Edited by:

Giuseppe Valacchi,
University of Ferrara, Italy

Reviewed by:

Jan Nilsson,
Lund University, Sweden
Madeline Nieves-Cintrón,
University of California, Davis,
United States

***Correspondence:**

Tai-Ping Fan
tpf1000@cam.ac.uk
Andreas Bender
ab454@cam.ac.uk

†Present address:

Ran Joo Choi,
Department of Neurosurgery,
Brain Tumor Center, Severance
Hospital, Yonsei University College of
Medicine, Seoul, South Korea
Mohamad Zobir SZ,
Malaysian Institute of Pharmaceuticals
and Nutraceuticals IPHarm, National
Institutes of Biotechnology Malaysia,
Ministry of Science, Technology and
Innovation, Pulau Pinang, Malaysia
Nitin Sharma,
Department of Tumor Biology, Institute
for Cancer Research, The Norwegian
Radium Hospital, Oslo, Norway

Specialty section:

This article was submitted to
Cardiovascular and Smooth Muscle
Pharmacology,
a section of the journal
Frontiers in Pharmacology

Received: 10 November 2020

Accepted: 11 January 2021

Published: 10 February 2021

Citation:

Choi RJ, Mohamad Zobir SZ,
Alexander-Dann B, Sharma N,
Ma MKL, Lam BYH, Yeo GSH,
Zhang W, Fan T-P and Bender A
(2021) Combination of Ginsenosides
Rb2 and Rg3 Promotes Angiogenic
Phenotype of Human Endothelial Cells
via PI3K/Akt and MAPK/
ERK Pathways.
Front. Pharmacol. 12:618773.
doi: 10.3389/fphar.2021.618773

Combination of Ginsenosides Rb2 and Rg3 Promotes Angiogenic Phenotype of Human Endothelial Cells via PI3K/Akt and MAPK/ERK Pathways

Ran Joo Choi^{1,2†}, Siti Zuraidah Mohamad Zobir^{1†}, Ben Alexander-Dann¹, Nitin Sharma^{1†}, Marcella K.L. Ma³, Brian Y.H. Lam³, Giles S.H. Yeo³, Weidong Zhang⁴, Tai-Ping Fan^{2*} and Andreas Bender^{1*}

¹Department of Chemistry, Center for Molecular Science Informatics, University of Cambridge, Cambridge, United Kingdom, ²Department of Pharmacology, University of Cambridge, Cambridge, United Kingdom, ³Medical Research Council (MRC) Metabolic Diseases Unit, University of Cambridge Metabolic Research Laboratories, Wellcome–MRC Institute of Metabolic Science, Genomics and Transcriptomics Core, Addenbrooke's Hospital, Cambridge, United Kingdom, ⁴Department of Pharmacy, Second Military Medical University, Shanghai, China

Shexiang Baoxin Pill (SBP) is an oral formulation of Chinese materia medica for the treatment of angina pectoris. It displays pleiotropic roles in protecting the cardiovascular system. However, the mode of action of SBP in promoting angiogenesis, and in particular the synergy between its constituents is currently not fully understood. The combination of ginsenosides Rb2 and Rg3 were studied in human umbilical vein endothelial cells (HUVECs) for their proangiogenic effects. To understand the mode of action of the combination in more mechanistic detail, RNA-Seq analysis was conducted, and differentially expressed genes (DEGs), pathway analysis and Weighted Gene Correlation Network Analysis (WGCNA) were applied to further identify important genes that play a pivotal role in the combination treatment. The effects of pathway-specific inhibitors were observed to provide further support for the hypothesized mode of action of the combination. Ginsenosides Rb2 and Rg3 synergistically promoted HUVEC proliferation and tube formation under defined culture conditions. Also, the combination of Rb2/Rg3 rescued cells from homocysteine-induced damage. mRNA expression of *CXCL8*, *CYR61*, *FGF16* and *FGFRL1* was significantly elevated by the Rb2/Rg3 treatment, and representative signaling pathways induced by these genes were found. The increase of protein levels of phosphorylated-Akt and ERK42/44 by the Rb2/Rg3 combination supports the notion that it promotes endothelial cell proliferation via the PI3K/Akt and MAPK/ERK signaling pathways. The present study provides the hypothesis that SBP, via ginsenosides Rb2 and Rg3, involves the CXCR1/2 CXCL8 (IL8)-mediated PI3K/Akt and MAPK/ERK signaling pathways in achieving its proangiogenic effects.

Abbreviations: SBP, shexiang baoxin pill; HUVECs, human umbilical vein endothelial cells; DEGs, differentially expressed genes; WGCNA, weighted gene correlation network analysis; TCM, traditional Chinese medicine; CHD, coronary heart disease; eNOS, endothelial nitric oxide synthase; MAPK, mitogen-activated protein kinase; GSEA, gene set enrichment analysis; HDFs, human dermal fibroblasts; HCY, homocysteine

Keywords: angiogenesis, tube formation, RNA-seq, weighted gene correlation network analysis, synergistic combination, shexiang baoxin pill, ginsenoside Rb2, ginsenoside Rg3

INTRODUCTION

Shexiang Baoxin Pill (SBP) is a traditional Chinese medicine (TCM) formulation taken orally to treat coronary heart disease (CHD) such as chronic stable angina (Lu et al., 2018). Like many other traditional medicines, SBP is derived from plant and animal products that contain a multitude of components which are thought to contribute to the holistic efficacy of the formulation (Yan et al., 2006; Yan et al., 2009). SBP has previously been shown to be protective against myocardial infarction (Wu et al., 2020) and associated oxidative injury and inflammation in rat models (Xiang et al., 2012; Xiang et al., 2013). Emerging pharmacological studies have revealed that SBP displays pleiotropic roles in protecting the cardiovascular system, as seen by the promotion of angiogenesis, amelioration of inflammation, improvement of endothelium dysfunction, mitigation of dyslipidemia, repression of vascular smooth muscle cell proliferation, and migration and restraint of cardiac remodeling (Lu et al., 2018).

On the mechanistic level, SBP has been shown to promote angiogenesis by stimulating proliferation, migration, and nitric oxide (NO) secretion by endothelial progenitor cells (Wu et al., 2009). According to a recent meta-analysis of 25 studies with 439 animals, SBP was shown to reduce myocardial infarction area through an increase of vascular endothelial growth factor (VEGF) and microvessel count in CHD, indicating that SBP's cardioprotective effects are largely due to promotion of angiogenesis (Zhang et al., 2017). In a rabbit model of myocardial infarction, administration of SBP enhances angiogenesis in the infarcted area, whilst reducing capillary density at the atherosclerotic plaque site in animal models at the same time (Shen et al., 2010). In a previous study, one of us has shown that the mixture of several compounds can show much the same effects compared to the SBP extract by analyzing microarray data (Fang et al., 2017). In this study, we tested the hypothesis that a limited number of compounds found in SBP can synergistically interact with each other to play a major role in treating cardiovascular diseases by promoting angiogenesis. Therapeutic angiogenesis is a heavily investigated and promising method for treatment of refractory angina or myocardial ischemia, among other indications (Attanasio and Schaer, 2011; Mitsos et al., 2012).

In order to investigate the pro-angiogenic effect of SBP and to understand its mechanism of action further, suitable model systems are needed. Endothelial cells (ECs) are the principal players involved in angiogenesis, and their ability to divide and differentiate into tube-like structures *in vitro* has long been a strong indicator of their key role in physiological and pathological angiogenesis (Munoz-Chapuli et al., 2004) and thus, ECs can be used in an *in vitro* model to study angiogenesis. ECs are highly responsive to signals such as VEGF and fibroblast growth factors (FGFs) (Carmeliet and Jain, 2011). The pro-angiogenic response often involves multiple steps, including Akt activation (Fang et al., 2013) as well as activation of its downstream target, endothelial nitric oxide synthase (eNOS). NO release is one of the first events in the angiogenic cascade, preceding new lumen

formation and even tip cell migration (Carmeliet and Jain, 2011). On the other hand, the mitogen-activated protein kinase (MAPK) pathway increases apoptotic pathway activated by environmental stressors that downregulates the pro-angiogenic VEGF pathway to mediate angiogenesis (Gomes and Rockwell, 2008), and accompanies serum-starved apoptosis in ECs (Yilmaz et al., 2003).

Human umbilical vein endothelial cells (HUVECs) are the most commonly used *in vitro* models of angiogenesis, where it is possible to observe their migration, proliferation and tubule formation in response to exogenous inhibitory or stimulatory agents (Staton et al., 2004). Overall, based on previous studies above, their frequent use as a model system, and their ability to recapitulate biologically relevant pathways (DeCicco-Skinner et al., 2014), we chose HUVECs in this work to untangle some aspects of the mode of action of angiogenesis modulators.

In a related study we modeled 22 chemicals identified in blood plasma after oral administration of SBP, and their ability in pairwise combinations to promote angiogenesis *in vitro* (Zobir et al., submitted). Here we systematically developed an algorithm to predict the synergy of all 231 pairwise combinations of those 22 compounds, which was also successfully experimentally validated. It was proposed from this previous work based on and *in silico* target prediction model that certain complementary pathways are responsible for the synergistic effect in promoting HUVEC proliferation. From the compound side, ginsenoside Rb2 in combination with ginsenoside Rg3 was found to dramatically increase proliferation of HUVECs, and protected these cells against homocysteine-induced damage. However, this previous study did not experimentally validate molecular mechanisms that caused those pro-angiogenic effects for this compound combination.

Hence, the present study aims to investigate the underlying mechanisms of the combination of ginsenosides Rg2 and Rg3 by utilizing RNA-sequencing (RNA-Seq) data generated in a biologically relevant system. The mRNA readout was analyzed by two standard methods in the field, namely Weighted Gene Co-expression Network Analysis (WGCNA) (Langfelder and Horvath, 2008) and Gene Set Enrichment Analysis (GSEA) (Subramanian et al., 2005), followed by expression validation using qPCR. In addition, we used pathway inhibitors to successfully verify the hypothesized modes of action, and applied phenotypic assays to further elucidate the mechanisms of this compound combination related to their modulation of angiogenic processes.

MATERIALS AND METHODS

General Materials and Cell Culture Ginsenosides

Ginsenoside Rb2 (purity >99.0%) was supplied by Shanghai Hutchison Pharmaceuticals Ltd. (Shanghai, China) (Fang et al., 2017), and ginsenoside Rg3 with >98.0% purity was

supplied by Prof. Yeong Shik Kim, Seoul National University, Republic of Korea (Ha et al., 2007). Compounds were dissolved to 100 mM in DMSO, then subsequently diluted in media. The final concentration of DMSO was less than 0.1%, which is not toxic to cells, and the vehicle control also contained the same amount of DMSO as the compound solution to identify any solvent-induced effects.

Cells and Biological Tools

HUVECs and human dermal fibroblasts (HDFs) were purchased from PromoCell (Heidelberg, Germany). Cells were cultured in PromoCell's Endothelial Cell Growth Medium 2 (EGM-2) containing 2% FBS, human epidermal growth factor (EGF), human basic fibroblast growth factor (FGF), insulin-like growth factor (IGF), human vascular endothelial growth factor 165 (VEGF₁₆₅), ascorbic acid and heparin. Trypsin 0.005%/EDTA 0.01% solution, Dulbecco A phosphate buffered saline (PBS) and 1-Step™ NBT/BCIP (Pierce Protein Research) were obtained from Thermo Fisher Scientific (MA, U.S.A.). Fetal bovine serum (FBS), dimethyl sulfoxide (DMSO), paraformaldehyde, Triton® X-100, rabbit anti-human von Willebrand factor antibody (F-3520), and mouse anti-rabbit IgG-alkaline phosphatase (A9919) were purchased from Sigma-Aldrich (Gillingham, United Kingdom). Human recombinant VEGF and precast gels were obtained from Invitrogen Life Technologies (Paisley, United Kingdom) and antibodies for Western blotting were sourced from Cell Signaling through New England Biolabs (Hitchin, United Kingdom).

Cell Viability Measurement

The effect of compounds and compound combinations on cell proliferation *in vitro* was assessed by the Cell Counting Kit-8 (CCK-8) assay (Dojindo, Kumamoto, Japan). CCK-8 utilizes the highly water-soluble tetrazolium salt WST-8, and dehydrogenases within living cells reduce WST-8 to produce colored (orange) formazan. The amount of formazan dye generated is then proportional to the number of living cells.

HUVECs were seeded onto 96-well flat-bottom plates at a density of 2.5×10^3 cells per well in 100 μ l of EGM-2. Following incubation for 24 h, the culture medium was aspirated and replaced with diluted drug solutions or vehicle controls in Endothelial Cell Basal Medium 2 (EBM-2, PromoCell). Combinations of ginsenoside Rb2 (10, 50, 100 μ M) and ginsenoside Rg3 (1, 5, 10 μ M) were treated in a 4×4 checkerboard arrangement allowing synergy to be quantified, and therefore the best pair of concentrations of each compound can be determined (Hsieh et al., 1993; Orhan et al., 2005; Vlot et al., 2019). After incubation for a further 72 h, 10 μ l of CCK-8 (Dijindo) was added to each well, and plates were incubated for 2 h in darkness at 37°C. Absorbance at 450 nm was then measured with a MultiSkan Ascent Plate Reader (MTX LAB SYSTEMS, Florida, U.S.A.).

For sulforhodamine B (SRB) assay, HUVECs were treated with drug solutions or vehicle controls under the same culture condition as above. After 72 h of incubation, media was removed and then cells were fixed in cold 3% Trichloroacetic acid (TCA)

for 30 min at 4°C. 0.057% SRB in 1% acetic acid were added to the cells and images were captured. The ImageJ software was used to count cell numbers present in each image.

Bliss Independence Model Measurement

The combination response (4×4) matrix contained percentages of cell growth, with cell growth without compound treatment set to 100%. Since the compounds applied either individually or in combination are assumed to promote cell growth, each value in the matrix was subtracted from 100 to produce percentage cell growth starting from 0%. A single-compound dose response curve was fitted to the data using the 4-parameter log-logistic function (4-PL) with the Synergy Finder package in R (R Development Core Team, 2010; He et al., 2018). Subsequently, the synergy of the combination was calculated using the Bliss model (Bliss, 1939), which assumes the drugs to act *via* independent mechanisms (For a discussion of the theoretical background and advantages and disadvantages of the different synergy models see a recent review (Vlot et al., 2019)). The Bliss score of the combination was calculated by averaging the difference between the actual percentage of cell growth and the expected percentage of cell growth with four replicate values, also in Synergy Finder.

IncuCyte Time-Lapse Imaging

Images were acquired with the IncuCyte Live Cell Imaging microscopy (Essen Bioscience) every 3 h up to 72 h under cell culture conditions with a 10X objective. Averaged cell confluence was calculated from three random fields of view per well using the IncuCyte in-built algorithm. Relative confluence values were obtained by normalizing each value to the time zero value in each sample.

Homocysteine-Induced Damage in a Co-culture Tube Formation Assay

The tube formation assay used here is based on the Bishop Model of co-culture tube formation (Bishop et al., 1999). Briefly, HUVECs and HDFs were cultured in EGM-2 until sub-confluent. Cells were then seeded in 48-well flat-bottom plates at a 1:20 ratio at around 2,000 HUVECs to 40,000 HDFs per well in EGM-2 medium. After two days, media were replenished, and on day 4, to allow for detection of protective effects of drugs against homocysteine (HCY)-induced damage, EGM-2 was titrated 10-fold with its basal medium (EBM-2) and 2% FBS. After 4 h of incubation with ginsenoside Rb2 (50 μ M) alone, ginsenoside Rg3 (5 μ M) alone, or the Rb2/Rg3 combination showing the highest Biliss synergy score, 2 mM HCY was added. These reagents in fresh media were replenished every two days before staining on day 12.

For staining, cells were first fixed and permeabilized with 4% paraformaldehyde in PBS, and an anti-human-vWF monoclonal antibody (dilution ratio 1:1,000; Sigma-Aldrich, MO, U.S.A.) was added (dilution ratio 1:1,000) for 1 h before staining with an anti-rabbit alkaline phosphatase conjugated antibody (dilution ratio 1:1,000) for 45 min. The 1-Step™ NBT/BCIP (Thermo Fisher Scientific, MA, U.S.A.) was applied until a suitable

signal was developed (10–15 min). Images of two fields of view were taken for three wells each, and total tube area measured using the ImageJ software. Total tube area was calculated as the number of connected pixels using “Analyze particles” above a certain size threshold (200-∞) following a binary normalization with an automatic threshold level.

RNA-Sequencing

Total RNA was isolated from cells using the RNeasy Kit (Qiagen) according to the manufacturer’s protocol. An additional DNaseI digestion step was performed to ensure that the samples were not contaminated with genomic DNA. One microgram of total RNA, after validation by an Agilent Bioanalyser 2,100 system to have an appropriate RIN between 7.6–10, was used for library construction using Illumina’s TruSeq Stranded mRNA Library Prep Kit (Illumina, CA, U.S.A) at the Institute of Metabolic Science Genomics and Transcriptomics Core Facility (Cambridge, United Kingdom). Messenger RNA was enriched by poly-T oligo attached magnetic beads before reverse transcription. Addition of a single “A” nucleotide (adenylation) after the synthesis of the double-stranded cDNA stopped the ligation of DNA fragments during the adapter ligation reaction. Unique barcodes were added to individual samples allowing multiplexed sequencing. DNA fragments with successful adapters ligated were enriched with a limited amplification. The second strand cDNA, with the incorporation of dUTP, was quenched during amplification to allow strand-specific sequencing. Indexed libraries were purified, normalized, pooled and sequenced on the Illumina HiSeq 4,000 platform at single read length of 50 base pairs at the Genomics Core Facility, Cancer Research United Kingdom Cambridge Institute (Cambridge, United Kingdom). The raw count data can be found at the following link <https://www.ncbi.nlm.nih.gov/Traces/study/?acc=PRJNA671806>.

Analysis of Differentially Expressed Genes

The quality of the reads was examined using FastQC (Andrews, 2010) and Trimmomatic (Bolger et al., 2014). An index for the reference genome, GRCh38 (Kersey et al., 2016) was created using Bowtie2 (Langmead and Salzberg, 2012). Reads were then mapped to the reference genome using Tophat2 (Kim et al., 2013) with the --b2-very-sensitive option. HTSeq-0.6 (Anders et al., 2015) was used to count the number of reads sorted by read name using SAMtools (Li et al., 2009). Differentially expressed genes (DEGs) between the untreated control and compound-treated groups were estimated using the DESeq2 statistical package (Love et al., 2014) with significant genes defined as those with a False Discovery Rate (FDR) ≤ 0.01 .

Weighted Correlation Network Analysis

The reads were matched to genes using the AnnotationDbi (Pagès et al., 2018) and org.Hs.eg.db (Carlson, 2019) packages in R (version 3.5.1) (R Core Team, 2018). Genes with zero variance across all samples (control as well as Rb2, Rg3, Rb2+Rg3 and FGF-treated) were removed. The remaining samples were hierarchically clustered using average linkage and Euclidean distance across all genes in R using the “wgcn” package (Langfelder and Horvath, 2008). The unsigned network was

built using correlation of genes with the parameters softpower $\beta = 10$, mergeCutHeight = 0.15, detectCutHeight = 0.995, and maxBlockHeight = 32,000. Module size has a positive correlation with Zsummary, a score that determines module preservation (Langfelder et al., 2011). Choosing a larger number of similarly sized modules allows for a fair comparison of the modules, and hence was used for subsequent analysis. A Fisher’s Exact Test was performed in WGCNA package to measure the categorical overlap between the resultant modules. Module preservation and reproducibility were determined using a permutation of the inner- and intra-connectivity, eigengenes and densities between the compound induced and control networks (Langfelder et al., 2011), resulting in Zsummary scores and median ranks. A previously suggested cutoff (Langfelder et al., 2011) of Zsummary scores >10 for strong evidence of conservation was applied, and 15 modules were excluded as these were not significantly conserved when compared to the control group (and so are assumed to represent unperturbed biological mechanisms). Genes were filtered for intramodular correlation (>0.7) and significance (<0.01) to focus on genes that are central to the modules, in the connectivity space. In this manner, the remaining genes are significantly correlated to the module, and so increases the likelihood that they are assigned to the correct module.

Gene Set and Pathway Analysis

Gene sets were analyzed using DAVID v 6.8 (Huang et al., 2009b; a) to determine enriched Gene Ontology (GO) Biological Processes of differentially expressed genes in the combination-treated group, compared to control and highly enriched pathways (p value <0.05) were identified with their constituent genes. DAVID analysis was conducted under medium stringency for biological process enrichment (Category: GOTERM_BP_DIRECT) and annotation clusters were summarized manually for representation purposes. To detect overrepresentation of genes in canonical pathways, differentially expressed genes were compared to the background of all measure genes. Genesets used were the Molecular Signatures database v 6.1 (Subramanian et al., 2005) (<http://www.broadinstitute.org/gsea/msigdb/index.jsp>), and overlap of genes in a pathway level interaction network was conducted with the ConsensusPathDB release 30 (January 09, 2015).

Quantitative Real Time PCR

A manually selected subset of genes of particular interest originating from the above analyses (pathway annotation and WGCNA analysis of RNA-seq results) were validated experimentally through quantitative real-time polymerase chain reaction (qPCR). Specific primers for selected genes were designed according to literature (Supplementary Table S2). All samples were amplified in triplicates and RNA utilized for real-time qPCR was extracted with RNeasy as described above. Purified RNA was reverse transcribed using the iScript™ cDNA Synthesis Kit (BIO-RAD) following the manufacturer protocol. Real time PCR amplifications were performed in Quantstudio 5 (Thermo Fisher Scientific, MA, U.S.A.) with an initial hot start of 95°C for 15 min followed by 45 cycles of 95°C for 15 s and 60°C for 30 s. In order to normalize

qPCR reactions, GAPDH (Glyceraldehyde 3-phosphate dehydrogenase) was included as housekeeping gene. The relative expression of genes was calculated based on the average Ct values across samples and significance was determined using the Students *t*-test (Microsoft Excel 2019, Microsoft, WA, U.S.A.), comparing control vs. the combination-treated mean values.

Western Blotting

Western blots were performed on HUVECs grown in 6-well plates. Following 30 min of incubation with drug or vehicle total cell protein was harvested using a lysis buffer (50 mM Tris-HCl, pH 7.5, 250 mM NaCl, 5 mM EDTA, 50 mM sodium fluoride, 0.5% sodium deoxycholate, 0.5% Triton X-100, protease inhibitor cocktail) and protein concentration was measured using the BCA Protein Assay Kit (Pierce Protein Research, Thermo Fisher Scientific, MA, U.S.A.). Equal amounts of protein were loaded into a 4–12% Bis-Tris gel (Invitrogen, Paisley United Kingdom) before being transferred onto a nitrocellulose membrane (Thermo Fisher Scientific, MA, U.S.A.). The membranes were blocked in TBS-T + 5% milk and then stained using primary antibodies (dilution ratio 1:1,000) overnight at 4°C, or at room temperature for 1 h with gentle shaking in TBS-T solution. Following three washes, horseradish peroxidase-conjugated secondary antibody (rabbit anti-mouse, 1:5,000) was added for 1 h at room temperature with gentle shaking. The signal was developed using Amersham ECL Prime (GE Healthcare, Buckinghamshire United Kingdom).

Statistical Analysis

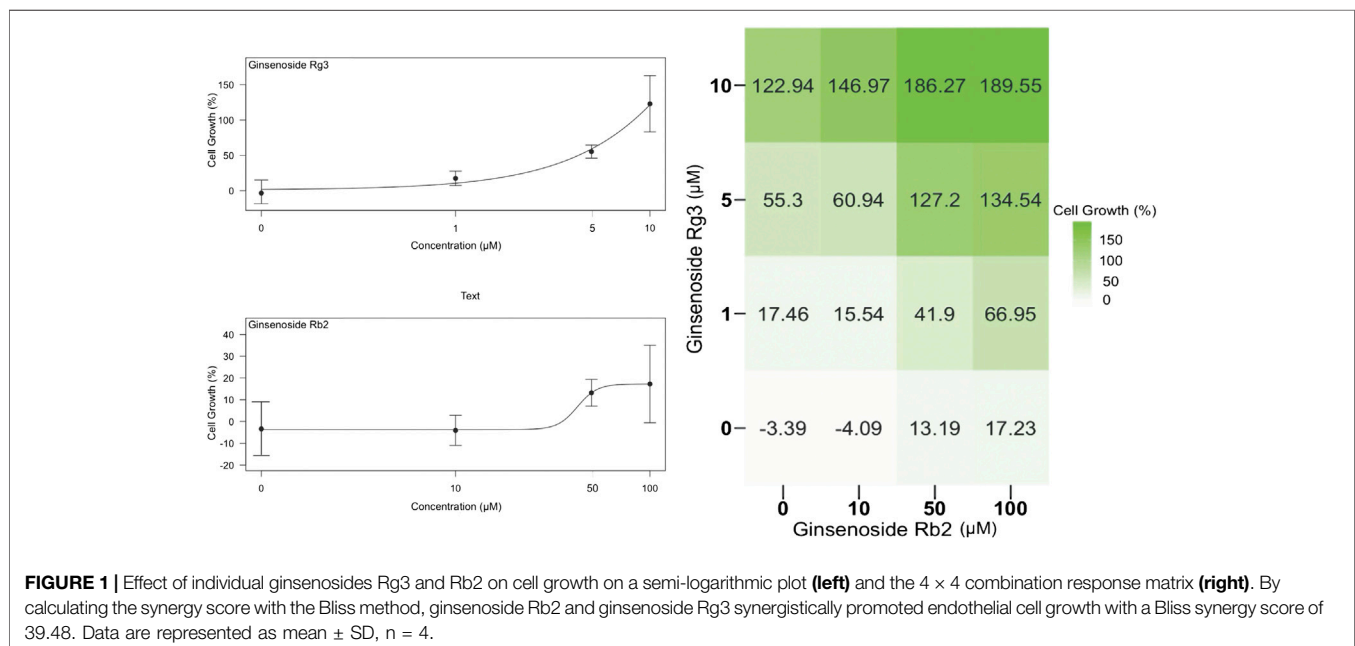
An ordinary one-way ANOVA with a Tukey's multiple comparisons test or a non-parametric Kruskal–Wallis one-way analysis was performed on cell-based *in vitro* data using GraphPad Prism version five for Windows (GraphPad

Software, CA, USA, www.graphpad.com), where the mean of each treatment group was compared with the mean of the control. $p < 0.05$ were considered as statistically significant.

RESULTS

Synergistic Effects of Ginsenosides Rb2 and Rg3 on Promoting Endothelial Cell Proliferation

We first sought to characterize the effects of each single ginsenoside on HUVEC proliferation to determine the optimal concentration range for experiments. Since ginsenoside Rg3 is known to show cell cytotoxicity at higher doses and thus widely used in cancer treatments (Joo et al., 2015), we decided to use concentrations of 10–100 μ M for ginsenoside Rb2 and 1–10 μ M for ginsenoside Rg3 individually as well as in a 4 × 4 concentration matrix (**Figure 1**). On the left side, individual effects of ginsenoside Rb2 or ginsenoside Rg3 on HUVEC proliferation were shown. Both compounds have enhancing effects over the basal growth, notably ginsenoside Rg3 promotes cell proliferation from 20% at 1 μ M to 120% at 10 μ M, whereas ginsenoside Rb2 produced a weaker proliferating effect, showing a sigmoidal curve. On the right side of **Figure 1**, the percentage of the increase in cell proliferation can be seen in a checkerboard format with concentrations of each compound on X and Y axis. A Bliss (Bliss, 1939) synergy score of 39.48 was obtained in combination-treated cells (**Figure 1**) which strongly supported that ginsenoside Rb2 and ginsenoside Rg3 synergistically promote endothelial cell proliferation. A Bliss synergy score above 0 indicates synergism throughout the pairwise concentrations tested, thus 39.48 provides strong support to suggest that ginsenoside Rb2 and ginsenoside Rg3 can be a good combination in terms of promoting endothelial cell proliferation.



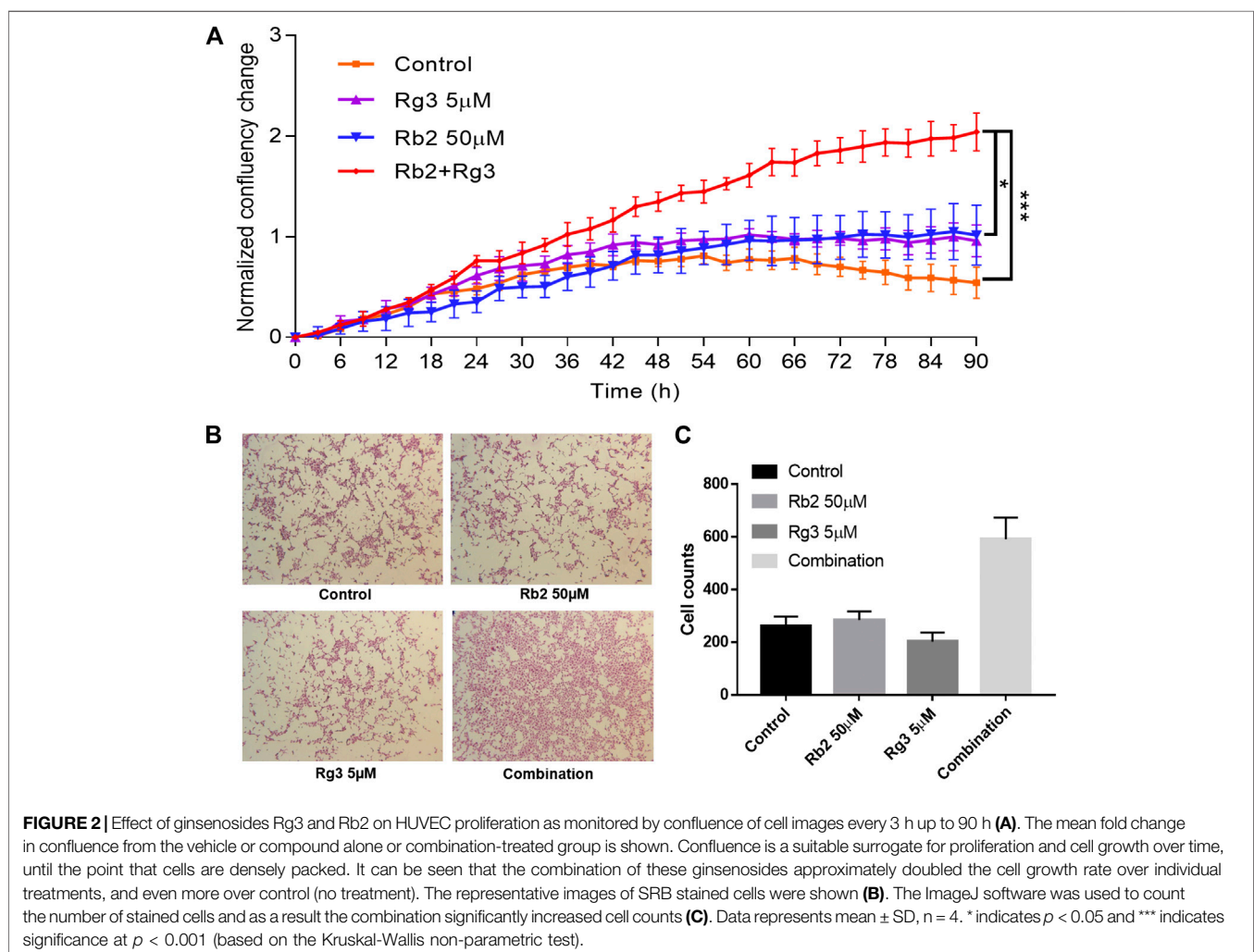
To investigate the time course of the synergistic effects of the combination of ginsenosides Rb2 (50 μM) and Rg3 (5 μM) on HUVEC growth, the IncuCyte system was used to track confluency changes. Since drugs were dissolved in medium without growth factors and nutrients the cell growth rate in the control wells was slightly decreased over time (Figure 2A). On the other hand, it was found that the cell population was increased 2-fold at 72 h compared to time zero by the combination of both ginsenosides, compared to either single agent or vehicle control (with $p < 0.001$, Figure 2). The results show that the combination of ginsenosides Rb2 and Rg3 can act like a replacement for essential growth supplements to promote cell proliferation when HUVECs are starved.

To add more convincing results, the SRB assay data were included in Figure 2. Representative images of stained cells after washout of floating cells in each group were shown in Figure 2B. Notably, the combination of Rb2 50 μM and Rg3 5 μM significantly promoted HUVEC cell growth (Figure 2C). The CCK-8 assay, the IncuCyte Live Cell Imaging and the SRB array differ in how they count the cell number, therefore the readouts of each method can vary. From the collection of obtained results, it is confirmed that the combination

showed ability to increase cell growth compared to either the vehicle control or the single treated group.

Ginsenosides Rb2 and Rg3 Protect Human Umbilical Vein Endothelial Cells Against Homocysteine-Induced Damage in a Co-culture Tube Formation Model

We next investigated the ability of endothelial cells to remodel and align *via* an *in vitro* tube formation assay, which is a requirement for the formation of new blood vessels during angiogenesis (Bishop et al., 1999). This method follows the interactions between endothelial cells and fibroblasts over 12 days leading to formation of vascular tubes with lumen and varying lengths, and is hence considered a better proxy (Gagnon et al., 2002) for the *in vivo* situation than the 6-h Matrigel method (Staton et al., 2004). Adding HCY to this co-culture tube formation model enables us to predict the ability of drugs to protect blood vessels against damage elicited by hyperhomocysteinemia. In the vehicle control group, co-culture of HUVECs and fibroblasts successfully formed vascular tubes which look like black thread, whilst 2 mM HCY destructed them. However,



when the positive control FGF was treated before HCY induction, tube-like structures were still formed, indicating FGF had ability to protect HCY-induced vascular damage (Figure 3). Likewise, the combination of 50 μ M ginsenoside Rb2 and 5 μ M ginsenoside Rg3 (with highest Bliss synergy) clearly protected HUVEC tube-like structures against 2 mM HCY-induced damage and hence reversed the damaged phenotype. Quantitative measure of areas of tube-like structures was conducted to confirm the protective effect of the combination and presented as a bar graph in Figure 3.

Distinct Gene Expression Patterns of Human Umbilical Vein Endothelial Cells Treated With Ginsenosides Rb2 and Rg3

We next analyzed the gene expression profile of HUVECs treated with either ginsenoside Rb2 (50 μ M), ginsenoside Rg3 (5 μ M) or Rb2/Rg3 combination in comparison to vehicle

control in order to elucidate the mechanistic basis of compound synergy. This analysis resulted in 377 and 45 significantly differently expressed genes (DEGs; FDR < 0.01) in the combination-treated group and the ginsenoside Rb2-treated group, respectively, compared to control, while no significant DEGs was observed on treatment of Rg3. Hence, on the overall level, when ginsenosides Rb2 and Rg3 are applied jointly, many more genes are altered than the sum of genes perturbed by the individual ginsenoside treatments, indicating compound interactions beyond simple additivity.

The 377 DEGs in the combination-treated cells were next subjected to Gene Set Enrichment Analysis (Subramanian et al., 2005), and the resulting ten highly enriched pathways with lowest *p* value are presented in Table 1. Extracellular matrix-related pathways are seen to be differentially regulated, indicating the pro-angiogenic effects by ginsenoside Rb2/Rg3 are at least partially due to extracellular matrix modulation (Sottile, 2004).

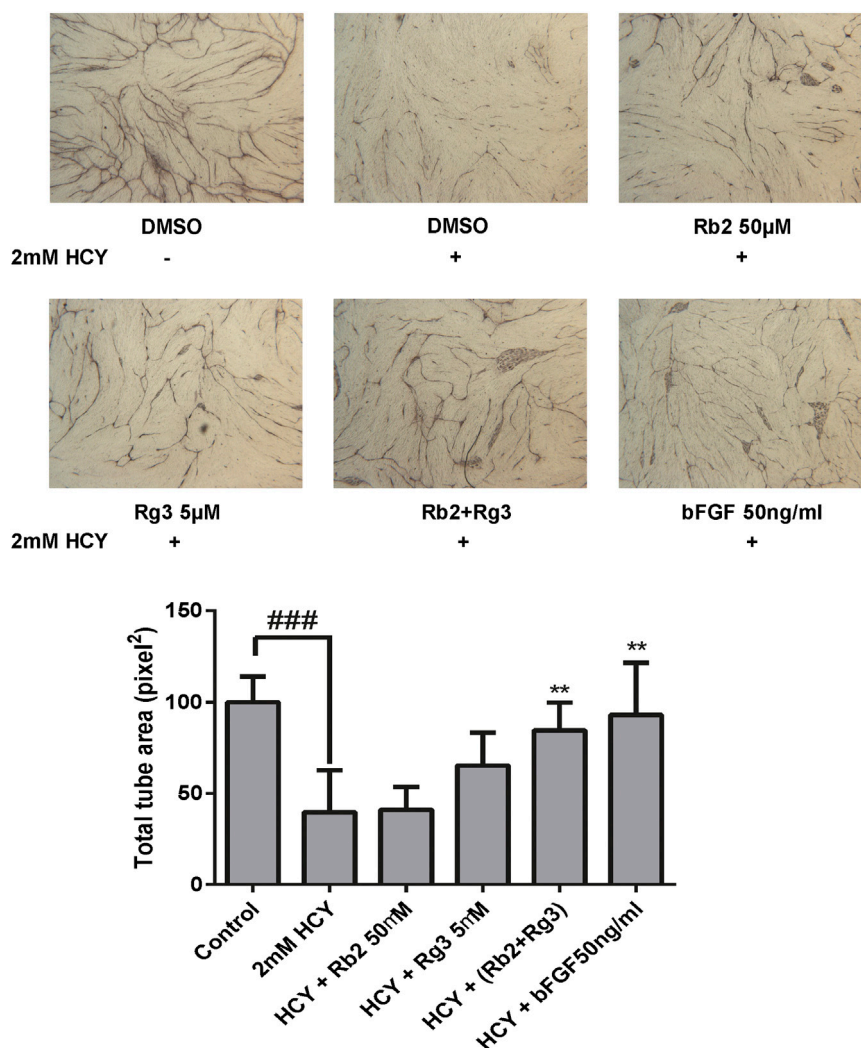


FIGURE 3 | The combination of ginsenosides Rb2 and Rg3 protected endothelial cell tube against homocysteine (HCY)-induced damage in a co-culture tube formation model. The protective effect of the ginsenoside Rb2/Rg3 combination was as good as the positive control FGF. Data represents mean \pm SD (*n* = 3). ### indicates *p* < 0.001; ** indicates *p* < 0.01 for treatment rescue compared to homocysteine-induced damage (based on tukey's one-way ANOVA).

Next, we conducted Consensus PathDB (Kamburov et al., 2013) for the 377 DEGs to obtain an alternative view on this information, such as interactions between pathways. The 10 most highly enriched pathways are listed in **Table 2** and visualized as a pathway level interaction network in **Figure 4**. Highly enriched pathways can be seen to be associated with cell growth and cell differentiation such as the EGFR, PDGFR and AP1 pathways, which hence form the mode of action hypothesis for angiogenesis modulation based on this part of the analysis. Ginsenoside Rb2 has been reported to promote epidermal proliferation via enhancing EGFR-related growth factors (Choi, 2002). Given that EGFR and PDGF are known receptors to promote angiogenesis, and AP1 families are important transcription factors to increase cell proliferation, we expect that the combination of ginsenoside Rb2 and Rg3 may target one or more of these pathways to produce overall effects.

Weighted Gene Correlation Network Analysis

Initially, all cases datasets—FGF treated positive control, individual Rb2 and Rg3 treatments, Rb2/Rg3 combination treatment and vehicle control - were hierarchically clustered in gene expression space (shown in **Supplementary Figure S1**). This separated FGF-induced cells from the others, suggesting a separate mode-of-action, which was to be expected as a positive control.

We next applied WGCNA to create modules of co-expressed genes for the combination-treated group and tested these modules based on their conservation against control networks, the results of which are shown in **Supplementary Table S1**. 78 modules were found to not be conserved against control. Networks were created for each condition and modules formed at four levels, with each level representing cutting the

tree at different heights (**Supplementary Figure S2**). Level 4, the lowest cut level, contained the large number (93) of distinct and specific modules compared to the other levels (which provided 56, 52, and 38 modules, respectively). The white module was both perturbed (i.e. not conserved) and contained the largest number of DEGs (**Supplementary Figure S3**). The combination of genes that are both differentially expressed and that are co-expressed (in the same module) could suggest the genes mutual involvement in the mode-of-action. Hence the white module was selected for further study.

All modules were then annotated with GO terms and, for example, the white module was found to have “angiogenesis (GO:0001525)” among its significant terms (**Table 3**). As shown in **Figure 5**, we conducted DESeq2 and WGCNA in parallel using RNA-seq data. By WGCNA, we found modules that shared no co-expression networks between control and treated groups and created 96 modules (deep split3) for the control and the combination groups. As a result, the white module showed the most significantly different co-expression between two groups (Seumois et al., 2016). In **Table 4**, the first six genes were selected because they were suggested by the WGCNA method with GO annotation (White GO module), while the remaining 12 genes were identified by DESeq2 in combination with either GSEA or CPDB pathway analysis.

Genes related to angiogenesis and cell proliferation and migration (GO terms GO:0001525, GO:0090050, GO:0008543), from the white module were selected for further study since they are most related to the observed activities we are interested in. Six genes from the white module have been suggested as central genes (high and significant correlation to module average) (**Table 4**), and five of them, except SERPINE1, are only suggested by WGCNA, (i.e. are not differentially expressed compared to control in an enriched gene set). In total, 18 genes were selected for further study (**Table 4**). We can see that different

TABLE 1 | Canonical pathways differentially expressed by Rb2/Rg3 combination treatment according to GSEA analysis (10 pathways with lowest *p*-value are shown).

Gene Set Name	# Genes in Gene Set (<i>K</i>) ¹	Description	# Genes in Overlap (<i>k</i>) ²	<i>k</i> / <i>K</i> ³	<i>p</i> -value	FDR <i>q</i> -value
NABA_MATRISOME	1,028	Ensemble of genes encoding extracellular matrix and extracellular matrix-associated proteins	49	0.0477	2.42×10^{-24}	3.22×10^{-21}
REACTOME_HEMOSTASIS	466	Genes involved in hemostasis	26	0.0558	5.76×10^{-15}	3.65×10^{-12}
NABA_MATRISOME_ASSOCIATED	753	Ensemble of genes encoding ECM-associated proteins including ECM-affiliated proteins, ECM regulators and secreted factors	32	0.0425	8.24×10^{-15}	3.65×10^{-12}
KEGG_FOCAL_ADHESION	201	Focal adhesion	17	0.0846	4.27×10^{-13}	1.42×10^{-10}
PID_FRA_PATHWAY	37	Validated transcriptional targets of AP1 family members Fra1 and Fra2	9	0.2432	8.65×10^{-12}	2.30×10^{-9}
NABA_SECRETED_FACTORS	344	Genes encoding secreted soluble factors	19	0.0552	3.32×10^{-11}	7.36×10^{-9}
KEGG_CYTOKINE_CYTOKINE_RECEPTOR_INTERACTION	267	Cytokine-cytokine receptor interaction	17	0.0637	4.03×10^{-11}	7.65×10^{-9}
NABA_CORE_MATRISOME	275	Ensemble of genes encoding core extracellular matrix including ECM glycoproteins, collagens and proteoglycans	17	0.0618	6.39×10^{-11}	1.06×10^{-8}
KEGG_PATHWAYS_IN_CANCER	328	Pathways in cancer	18	0.0549	1.22×10^{-10}	1.81×10^{-8}
PID_INTEGRIN3_PATHWAY	43	Beta3 integrin cell surface interactions	8	0.186	1.28×10^{-9}	1.71×10^{-7}

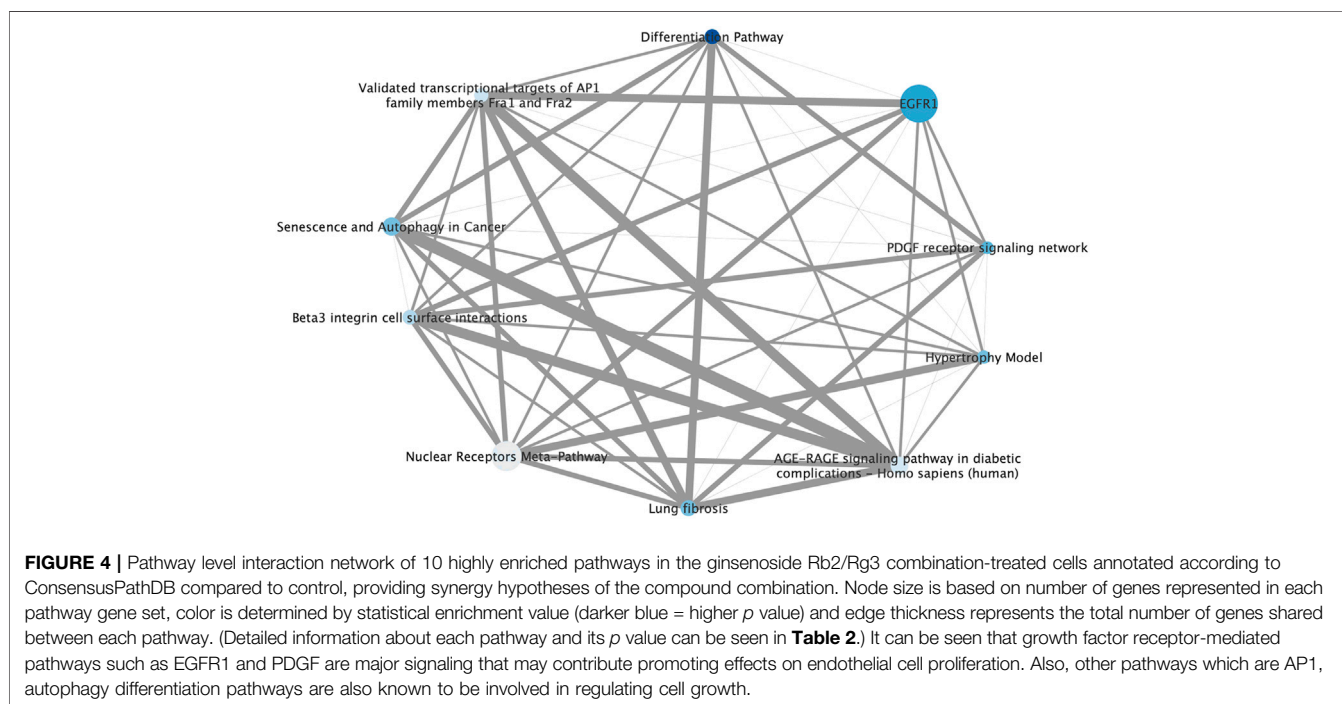
¹total number of genes in each gene set (*K*)

²number of genes of our DEGs in each gene set (*k*)

³ratio of *k* to *K*

TABLE 2 | Overrepresentation analysis using Consensus PathDB comparing differentially expressed genes in ginsenoside Rb2/Rg3 combination treated cells to control (10 pathways with lowest *p*-value are shown). Growth factor-involved signaling pathways, such as PDGF, EGFR1 and differentiation pathway, are overrepresented as well as cell survival pathways such as AP1, senescence and autophagy in cancer.

<i>p</i> -value	<i>q</i> -value	Pathway	Source
1.44×10^{-7}	0.000149	Validated transcriptional targets of AP1 family members Fra1 and Fra2	Pathway interaction database (PID) Schaefer et al. (2009)
8.07×10^{-7}	0.000417	Senescence and autophagy in cancer	Wikipathways Kelder et al. (2009)
3.34×10^{-6}	0.000856	AGE-RAGE signaling pathway in diabetic complications - homo sapiens (human)	KEGG Kanehisa and Goto (2000)
3.96×10^{-6}	0.000856	PDGF receptor signaling network	PID
4.15×10^{-6}	0.000856	Hypertrophy model	Wikipathways
5.11×10^{-6}	0.000879	Beta3 integrin cell surface interactions	PID
6.06×10^{-6}	0.000893	EGFR1	NetPath Kandasamy et al. (2010)
1.20×10^{-5}	0.00143	Differentiation pathway	Wikipathways
1.25×10^{-5}	0.00143	Nuclear receptors meta-pathway	Wikipathways
1.44×10^{-5}	0.00143	Lung fibrosis	Wikipathways



methods did not suggest entirely overlapping genes, for instance, only 10 DEGs are highly and significantly correlated in the white module. Thus, combining DEG and WGCNA approaches enables to search potential genetic biomarkers which may be overlooked when using only one method.

Gene Expression Analysis of Ginsenoside Rb2/Rg3 Combination Treatment Based on RNA-Seq and qPCR Data

We next performed quantitative polymerase chain reaction (qPCR) on the 18 selected genes (**Table 4**) after the combination treatment of ginsenoside Rb2 (50 μ M) and Rg3 (5 μ M). The quantitative fold change between the control and the combination-treated cells of mRNA expression as well as the result of RNA-Seq raw counts of the 18 genes were presented in

Figure 6. Notably, when compared with vehicle control, we can confirm that mRNA expression of *CXCL8*, *CYR61*, *FGF16* and *FGFRL1* was highly up-regulated by the Rb2/Rg3 combination.

The Ginsenoside Rb2/Rg3 Combination Acts via the CXCR1/2 CXCL8 (IL8)-Mediated PI3K/Akt and MAPK/ERK Signaling Pathways

To further explore the molecular basis of the pro-proliferative effect of the ginsenoside Rb2/Rg3 combination in HUVECs, the CXCR1/2 antagonist Reparixin, the ERK inhibitor U0126 and the PI3K inhibitor LY294002 were used to block their respective signaling cascades. U0126, a kinase inhibitor of ERK to prevent phosphorylation of ERK, a family of MAPK, has been used in HUVEC at 10 μ M in order to prove that their candidate drug

TABLE 3 | Gene Ontology analysis of Biological Processes of 94 genes found in the White Module, which is not conserved with the control network and contains the highest number of differentially expressed genes that correlated highly with the modules. It shows that this module is enriched in cell survival and angiogenesis signaling pathways, and hence these genes are of significant interest in determining the combination mode of action.

Term	Description	p-value
GO:0097191	Extrinsic apoptotic signaling pathway	0.0147
GO:0001525	Angiogenesis	0.0169
GO:0090050	Positive regulation of cell migration involved in sprouting angiogenesis	0.0304
GO:0008152	Metabolic process	0.0380
GO:0097105	Presynaptic membrane assembly	0.0390
GO:0070886	Positive regulation of calcineurin-NFAT signaling cascade	0.0390
GO:0043085	Positive regulation of catalytic activity	0.0496

induces angiogenesis via MAPK pathways (Wu et al., 2015). LY294002 blocks PI3K activity that phosphorylates Akt, resulting in unphosphorylated form of Akt. In this way we were able to test the hypothesis, based on mRNA analysis, that CYR61-stimulated IL-8 production leads to stimulation of the CXCR1/2 receptor, and thus the PI3K/Akt and MAPK/ERK signaling pathways are initiated consequently. The results of this experiment are shown in **Figures 7A–C** and demonstrate that the Rb2/Rg3-induced increase of HUVEC proliferation was significantly reduced in all three cases (and most pronouncedly by Reparixin), indicating that activation of CXCR1/2, MAPK/ERK and PI3K/Akt are involved in the mode of action of the combination. Western blot results (**Figure 7D**) demonstrated that Rb2/Rg3-induced Akt and ERK phosphorylation was significantly suppressed by LY294002 and U0126, while there was no reduction in the amount of total Akt and ERK protein present. This indicates that the activation of Akt and ERK *via* phosphorylation is also involved in the mode of action of the ginsenoside Rb2/Rg3 combination when stimulating HUVEC proliferation.

DISCUSSION

Shexiang Baoxin pill (SBP), which consists of seven materia medica, is widely used as a TCM formulation for the treatment of coronary heart disease. However, the modes of action of SBP in promoting angiogenesis have not yet been fully understood. In this regards, we previously modeled compound interactions of 22 constituent compounds detected in plasma (Zobir et al., submitted). However, while being able to predict synergies with a satisfactory performance and suggesting modes of action of compounds, this previous work did not biologically investigate mechanisms of synergistic interactions between compounds in promoting angiogenesis. Here, we focused on one particular combination of ginsenosides from SBP which has been identified as synergistic, that of ginsenosides Rb2 and Rg3, in order to investigate its molecular mode of action associated with angiogenesis.

Ginsenosides, isolated from *Panax ginseng*, are classified into two groups of saponins according to chemical structure: the dammarane-type having a 20(S)-protopanaxadiol/triol skeleton, and the oleanolic acid type possessing an oleanolic acid skeleton. Ginsenoside Rb2 and its hydrolytic product ginsenoside Rg3 belong to the protopanaxadiol type of dammarane ginsenosides. Ginsenosides Rb2 and Rg3 have multiple functions in immune regulation, anti-oxidation, anti-inflammation, anti-aging and anti-fatigue (Choi, 2002; Choi et al.,

2015; Joo et al., 2015; Kim et al., 2016; Sun et al., 2017). However, their pro-angiogenic effects have not been vigorously studied, while their anti-angiogenesis along with anti-tumorigenic effects have been shown in several cancers (Mochizuki et al., 1995; Joo et al., 2015; Sun et al., 2016; Sun et al., 2017). As one of the few examples, related to pro-angiogenic effects, Kim et al. reported that ginsenoside Rg3 at 1, 5, 10 μM was able to prevent INS-1 cell death by increasing cell proliferation (Kim et al., 2016). Likewise, in our experimental conditions using HUVECs, ginsenoside Rg3 at lower concentrations (below 10 μM) markedly increased HUVEC proliferation. It is notable that most of the anticancer effects of

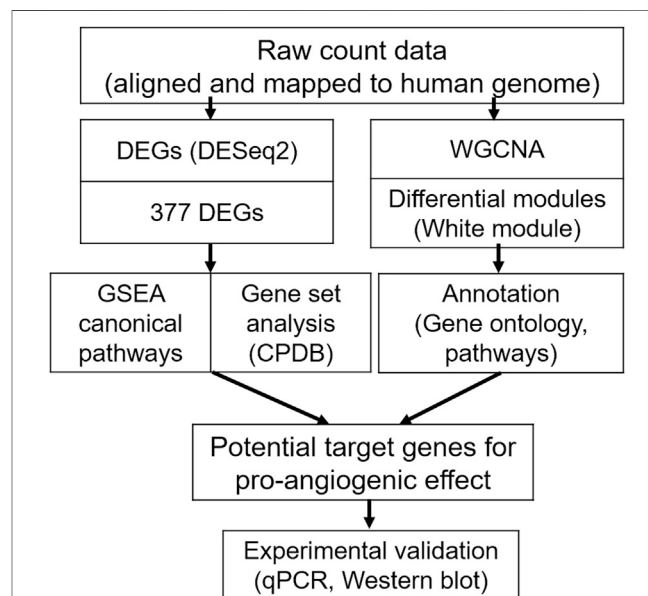


FIGURE 5 | Workflow of the RNA-sequencing (RNA-Seq) analysis for the ginsenoside Rb2/Rg3 combination, compared to the control group. Firstly (**left**), differentially expressed genes were determined using DESeq2. The 377 differentially expressed genes in the combination-treated group were subject to Gene Set Enrichment Analysis (GSEA) and Consensus Path DB (CPDB) gene set analyses. In parallel (**right**), Weighted Gene Co-expression Network Analysis (WGCNA) was performed on combination treated vs untreated cells, and the resulting white gene module was subject to Gene Ontology and pathway analysis. Both methods together were used to understand the synergistic effect of the ginsenoside combination treatment on a mechanistic level, and formed the basis of selecting 18 genes for further experimental validation by qPCR and Western blotting.

TABLE 4 | List of 18 genes selected from preceding analyses for confirmation by qPCR. The first six genes were suggested by the WGCNA method with GO annotation (White GO module), while the remaining 12 genes were identified by DESeq2 in combination with either GSEA or CPDB pathway analysis. Five genes (CIB1, MMP2, TNFRSF12A, FGF16, FGFR1) have been chosen by the WGCNA method only and not by DESeq2, indicating those genes from the most highly correlated module may still be important in angiogenesis pathways, despite not being significantly differentially expressed.

Gene symbol	Gene name	Module	Evidence
CIB1	Calcium and integrin binding 1	White	White GO
MMP2	Matrix metalloproteinase 2	White	White GO
SERPINE1	Serpin family E member 1	White	White GO/GSEA/CPDB
TNFRSF12A	TNF receptor superfamily member 12A	White	White GO
FGF16	Fibroblast growth factor 16	White	White GO
FGFR1	Fibroblast growth factor receptor-like 1	White	White GO
SPARC	Secreted protein acidic and cysteine rich	Purple	GSEA
PDGFA	Platelet derived growth factor subunit A	palevioletred3	GSEA/CPDB
SMOC1	SPARC related modular calcium binding 1	palevioletred2	GSEA
GDF3	Growth differentiation factor 3	navajowhite2	GSEA
TGFBR2	Transforming growth factor beta receptor 2	Lightyellow	GSEA/CPDB
PDGFRB	Platelet derived growth factor receptor beta	Darkmagenta	GSEA/CPDB
CYR61	Cysteine rich angiogenic inducer 61	Darkgrey	GSEA/CPDB
ITGB1	Integrin subunit beta 1	Black	GSEA
PDGFC	Platelet derived growth factor C	Black	GSEA
SLIT3	Slit guidance ligand 3	antiquewhite4	GSEA
IL8(CXCL8)	C-X-C motif chemokine ligand 8	Steelblue	GSEA/CPDB
EDN1	Endothelin 1	Steelblue	CPDB

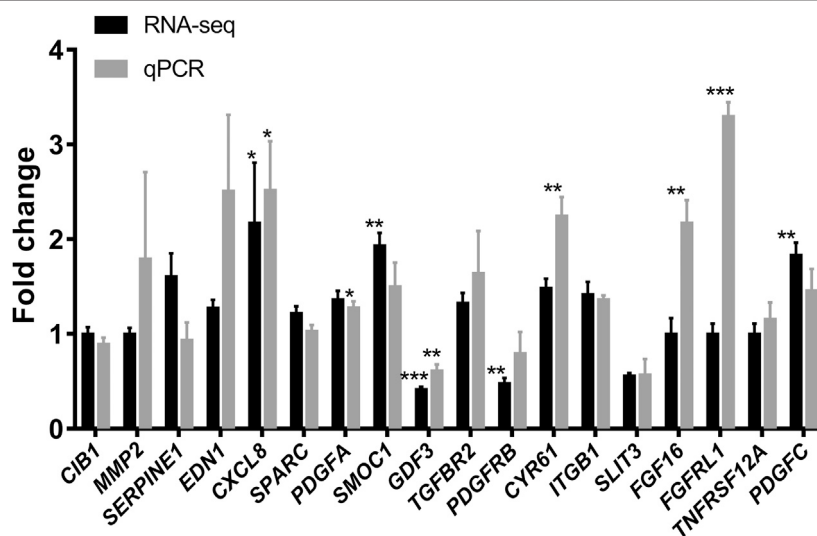
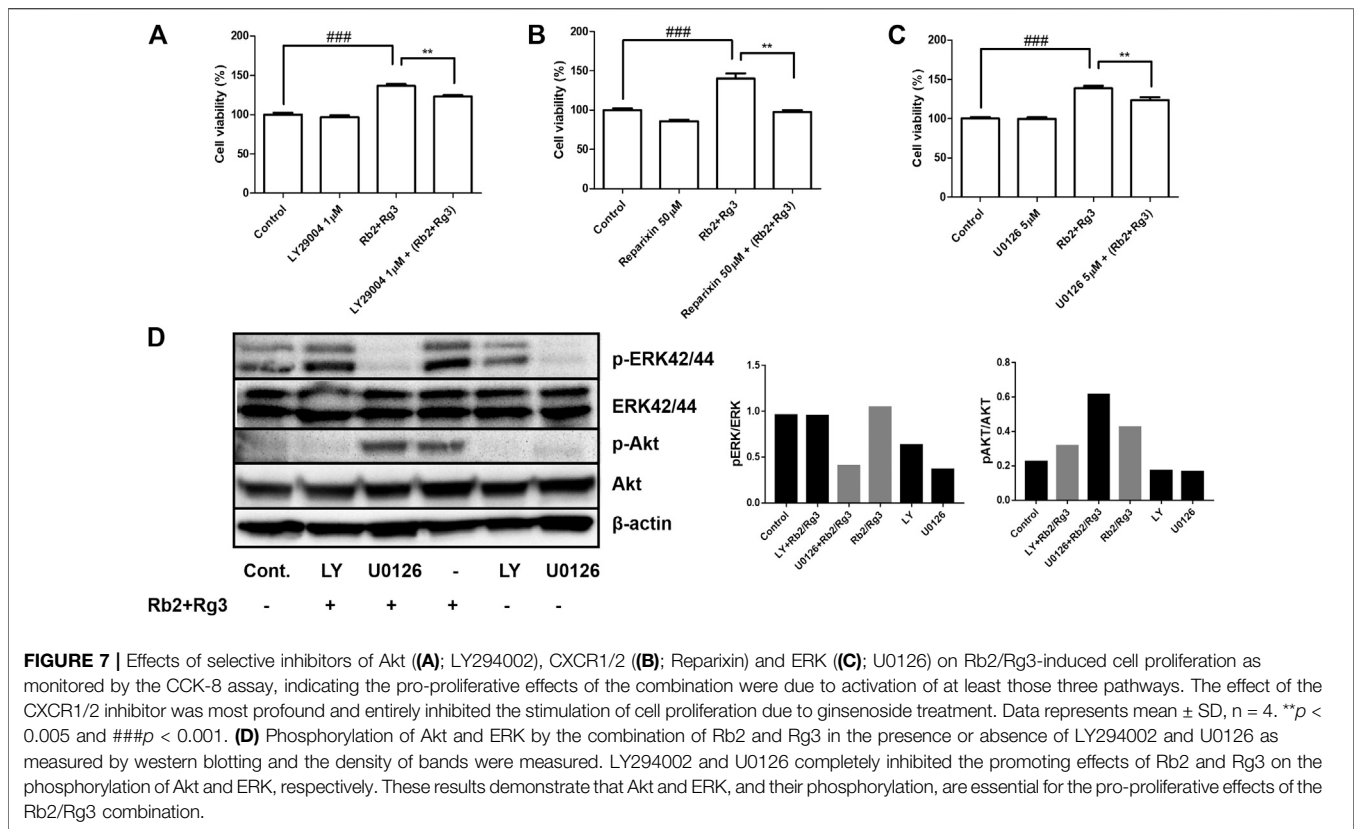


FIGURE 6 | Elevation of mRNA expression in HUVECs treated with the combination of ginsenoside Rb2 (50 μ M) and ginsenoside Rg3 (5 μ M) or vehicle for 72 h as determined by real time qPCR (in gray) and compared to RNA-Seq data (in black). It can be seen that the Rb2/Rg3 combination upregulated several genes by 2- to 3-fold, such as *CXCL8*, *CYR61*, *FGF16* and *FGFR1*. Data represents mean \pm SD of four replicates. * $p < 0.05$, ** $p < 0.01$, *** $p < 0.001$.

ginsenoside Rg3 have been observed at much higher concentrations (>25 μ M, although it varies on cell type). In addition, ginsenoside Rb2 has been reported that to enhance cell proliferation and migration by increasing EGF and EGFR levels (Choi, 2002). Given that ginsenosides have steroid-like structures, they are likely to bind to multiple steroid hormone receptors which may explain angiogenesis-modulating effects (Leung and Wong, 2010). Mechanisms of angiogenic activity of the saponin fraction has been proposed mainly through enhancement of tissue-type plasminogen activator (tPA) secretion together with suppression of plasminogen activator inhibitor-1 (PAI-1) secretion (Morisaki et al., 1995). Morisaki et al.

reasoned that ginsenosides resembling sterols may contribute to the angiogenic activity of saponin (Morisaki et al., 1995). Even though the effect of these ginsenosides under different conditions (cell/tissue type, concentration, etc.) is yet to be understood in detail, it is evident that they target angiogenesis, and hence this work aimed to understand the mode of action of two synergistic components of a relevant traditional Chinese medicine, SBP, in this context.

While most of combination therapy aims at inhibiting angiogenesis in cancer treatments, combination pharmacotherapy can also provide benefits to prevent cardiovascular disease both in patients with high risk factors and individuals with existing



cardiovascular disease (Working Group on the Summit on Combination Therapy for CVD et al., 2014). Our data demonstrate that a combination of ginsenosides Rb2 and Rg3 may act synergistically in promoting cellular proliferation as well as protecting endothelial cells from HCY-induced vascular damage. Ginsenoside Rb1, one of the protopanaxadiol type dammarane ginsenosides, has previously been shown to block HCY-induced endothelial dysfunction in porcine coronary arteries, suggesting potential clinical applications of ginsenosides in HCY-associated vascular injuries (Zhou et al., 2005). In our co-culture model of vascular tube formation, neither ginsenoside Rb2 alone nor ginsenoside Rg3 alone at the chosen concentrations was sufficient to rescue the tubes from HCY-induced damage; however, when combining these two ginsenosides together, the tube damage was largely reversed. The concentrations we used for the combination treatment were based on the Bliss synergy and the endothelial cell growth curves of each ginsenosides. Either ginsenoside Rb2 or ginsenoside Rg3 alone was able to show sigmoidal curves where the highest concentration hits plateau. Although synergism was observed throughout the areas of combination-treatments, ginsenoside Rb2 at 50 μ M combined with ginsenoside Rg3 at 5 μ M seem to be the best pair when compared to the single treatment.

In parallel with the potential therapeutic effects on reversing HCY-induced damage, the current study demonstrates that the ginsenoside Rb2/Rg3 combination can synergistically promote HUVEC proliferation. To elucidate the underlying molecular mechanism of the combination, RNA-Seq analysis of differentially expressed genes (DEGs) has been conducted in the present study. DEG analysis is a common method for

identifying genes that play an important role in phenotypic effects, while transcription factor modifications such as reversible phosphorylation and missense mutations can be overlooked (Langfelder et al., 2011). Therefore, WGCNA together with DEG approaches have been applied in order to understand the mode of action of the compound combination further. A total of 377 Rb2/Rg3-induced DEGs were found to be highly enriched with angiogenesis- and extracellular matrix-related pathways. Moreover, the module with highest overlap of highly correlating DEGs and not conserved with control by WGCNA was associated with angiogenesis-related biological processes, however identifying somewhat distinct individual genes, indicating the importance of using different analysis methods in parallel. Since applications of RNA-Seq are not completely known yet as according to the huge data generated, researchers face challenges to analyze to avoid sequencing artifacts. Therefore, combining two different tools provides us more confident outcomes that those selected genes are less likely artifacts but produced by meaningful biological processes.

Thus, in this study, we have provided the first evidence that ginsenoside Rb2 and ginsenoside Rg3 synergistically promote endothelial cell proliferation and protect them against HCY-induced damage. RNA-Seq data by DEG and WGCNA analysis further indicate that angiogenesis pathways are transcriptionally perturbed by the combination of ginsenosides Rb2 and Rg3. Confirmed by qPCR, Western blotting, and pathway inhibition experiments, we hence conclude that the Rb2/Rg3 combination promotes endothelial cell proliferation through the CXCR1/2 CXCL8 (IL8)-mediated PI3K/Akt and

MAPK/ERK signaling pathways (Heidemann et al., 2003) that may further effects on promoting angiogenesis.

More generally, the present study suggests a protocol on how to gain insight into the mode of action of a combination of two compounds from an originally more complex herbal formulation, which could be beneficial to standardize and simplify their complexity while maintaining efficacy.

DATA AVAILABILITY STATEMENT

The original contributions presented in the study are publicly available. This data can be found here: <https://www.ncbi.nlm.nih.gov/Traces/study/?acc=PRJNA671806>.

AUTHOR CONTRIBUTIONS

RC, SZ and BA designed the experiments and wrote the related studies. RC performed *in vitro* experiments and wrote the manuscript. MM, BL and GY performed RNA-

seq. BA and NS analyzed RNA-seq data and wrote the related parts. WZ provided related advices. TF and AB supervised the project and modified the manuscript. All authors have read and approved the final version of this manuscript.

FUNDING

The authors would like to thank the European Research Council (ERC Starting Grant to AB), the United Kingdom Medical Research Council (MRC) Metabolic disease Unit (MRC_MC_UU_00014/5), a Wellcome Trust Major Award (208363/Z/17/Z) and NSFC (81520108030).

SUPPLEMENTARY MATERIAL

The Supplementary Material for this article can be found online at: <https://www.frontiersin.org/articles/10.3389/fphar.2021.618773/full#supplementary-material>.

REFERENCES

- Anders, S., Pyl, P. T., and Huber, W. (2015). HTSeq—a Python framework to work with high-throughput sequencing data. *Bioinformatics* 31 (2), 166–169. doi:10.1093/bioinformatics/btu638
- Andrews, S. (2010). *RE: FastQC: a quality control tool for high throughput sequence data*. Berlin, Germany: ScienceOpen.
- Attanasio, S., and Schaer, G. (2011). Therapeutic angiogenesis for the management of refractory angina: current concepts. *Cardiovasc Ther.* 29 (6), e1–e11. doi:10.1111/j.1755-5922.2010.00153.x
- Bishop, E. T., Bell, G. T., Bloor, S., Broom, I. J., Hendry, N. F., and Wheatley, D. N. (1999). An *in vitro* model of angiogenesis: basic features. *Angiogenesis* 3 (4), 335–344. doi:10.1023/A:1026546219962
- Bliss, C. I. (1939). The toxicity of poisons applied jointly. *Ann. Appl. Biol.* 26 (3), 585–615. doi:10.1111/j.1744-7348.1939.tb06990.x
- Bolger, A. M., Lohse, M., and Usadel, B. (2014). Trimmomatic: a flexible trimmer for Illumina sequence data. *Bioinformatics* 30 (15), 2114–2120. doi:10.1093/bioinformatics/btu170
- Carlson, M. (2019). *Genome wide annotation for Human. R package version 3.8.2*. (*org.Hs.eg.db*).
- Carmeliet, P., and Jain, R. K. (2011). Molecular mechanisms and clinical applications of angiogenesis. *Nature* 473, 298–307. doi:10.1038/nature10144
- Choi, R. J., Wong, A. S. T., Jia, W., Chang, I.-M., Wong, R. N. S., Fan, T. P., et al. (2015). Ginseng: a panacea linking east asia and north America? *Science* 350 (6262), S54–S56.
- Choi, S. (2002). Epidermis proliferative effect of the Panax ginseng ginsenoside Rb2. *Arch. Pharm. Res.* 25 (1), 71–76. doi:10.1007/BF02975265
- DeCicco-Skinner, K. L., Henry, G. H., Cataisson, C., Tabib, T., Gwilliam, J. C., Watson, N. J., et al. (2014). Endothelial cell tube formation assay for the *in vitro* study of angiogenesis. *J. Vis. Exp.* 91, e51312. doi:10.3791/51312
- Fang, H. Y., Zeng, H. W., Lin, L. M., Chen, X., Shen, X. N., Fu, P., et al. (2017). A network-based method for mechanistic investigation of Shexiang Baoxin Pill's treatment of cardiovascular diseases. *Sci. Rep.* 7, 43632. doi:10.1038/srep43632
- Fang, L., Choi, S. H., Baek, J. S., Liu, C., Almazan, F., Ulrich, F., et al. (2013). Control of angiogenesis by AIBP-mediated cholesterol efflux. *Nature* 498 (7452), 118–122. doi:10.1038/nature12166
- Gagnon, E., Cattaruzzi, P., Griffith, M., Muzakare, L., LeFlao, K., Faure, R., et al. (2002). Human vascular endothelial cells with extended life spans: *in vitro* cell response, protein expression, and angiogenesis. *Angiogenesis* 5 (1–2), 21–33. doi:10.1023/a:1021573013503
- Gomes, E., and Rockwell, P. (2008). p38 MAPK as a negative regulator of VEGF/VEGFR2 signaling pathway in serum deprived human SK-N-SH neuroblastoma cells. *Neurosci. Lett.* 431 (2), 95–100. doi:10.1016/j.neulet.2007.11.068
- Ha, Y. W., Lim, S. S., Ha, I. J., Na, Y. C., Seo, J. J., Shin, H., et al. (2007). Preparative isolation of four ginsenosides from Korean red ginseng (steam-treated Panax ginseng C. A. Meyer), by high-speed counter-current chromatography coupled with evaporative light scattering detection. *J. Chromatogr. A* 1151 (1–2), 37–44. doi:10.1016/j.chroma.2007.01.038
- He, L., Kuleskiy, E., Saarela, J., Turunen, L., Wennerberg, K., Aittokallio, T., et al. (2018). Methods for high-throughput drug combination screening and synergy scoring. *Methods Mol. Biol.* 1711, 351–398. doi:10.1007/978-1-4939-7493-1_17
- Heidemann, J., Ogawa, H., Dwinell, M. B., Rafiee, P., Maaser, C., Gockel, H. R., et al. (2003). Angiogenic effects of interleukin 8 (CXCL8) in human intestinal microvascular endothelial cells are mediated by CXCR2. *J. Biol. Chem.* 278 (10), 8508–8515. doi:10.1074/jbc.M208231200
- Hsieh, M. H., Yu, C. M., Yu, V. L., and Chow, J. W. (1993). Synergy assessed by checkerboard. A critical analysis. *Diagn. Microbiol. Infect. Dis.* 16 (4), 343–349. doi:10.1016/0732-8893(93)90087-n
- Huang, da. W., Sherman, B. T., and Lempicki, R. A. (2009a). Bioinformatics enrichment tools: paths toward the comprehensive functional analysis of large gene lists. *Nucleic Acids Res.* 37 (1), 1–13. doi:10.1093/nar/gkn923
- Huang, da. W., Sherman, B. T., and Lempicki, R. A. (2009b). Systematic and integrative analysis of large gene lists using DAVID bioinformatics resources. *Nat. Protoc.* 4 (1), 44–57. doi:10.1038/nprot.2008.211
- Joo, E. J., Chun, J., Ha, Y. W., Ko, H. J., Xu, M. Y., and Kim, Y. S. (2015). Novel roles of ginsenoside Rg3 in apoptosis through downregulation of epidermal growth factor receptor. *Chem. Biol. Interact.* 233, 25–34. doi:10.1016/j.cbi.2015.03.016
- Kamburov, A., Stelzl, U., Lehrach, H., and Herwig, R. (2013). The ConsensusPathDB interaction database: 2013 update. *Nucleic Acids Res.* 41 (Database issue), D793–D800. doi:10.1093/nar/gks1055
- Kandasamy, K., Mohan, S. S., Raju, R., Keerthikumar, S., Kumar, G. S., Venugopal, A. K., et al. (2010). NetPath: a public resource of curated signal transduction pathways. *Genome Biol.* 11 (1), R3. doi:10.1186/gb-2010-11-1-r3
- Kanehisa, M., and Goto, S. (2000). KEGG: kyoto encyclopedia of genes and genomes. *Nucleic Acids Res.* 28 (1), 27–30. doi:10.1093/nar/28.1.27
- Kelder, T., Pico, A. R., Hanspers, K., van Iersel, M. P., Evelo, C., and Conklin, B. R. (2009). Mining biological pathways using WikiPathways web services. *PLoS One* 4 (7), e6447. doi:10.1371/journal.pone.0006447
- Kersey, P. J., Allen, J. E., Armean, I., Boddie, S., Bolt, B. J., Carvalho-Silva, D., et al. (2016). Ensembl Genomes 2016: more genomes, more complexity. *Nucleic Acids Res.* 44 (D1), D574–D580. doi:10.1093/nar/gkv1209

- Kim, D., Pertea, G., Trapnell, C., Pimentel, H., Kelley, R., and Salzberg, S. L. (2013). TopHat2: accurate alignment of transcriptomes in the presence of insertions, deletions and gene fusions. *Genome Biol.* 14 (4), R36. doi:10.1186/gb-2013-14-4-r36
- Kim, Y. J., Park, S. M., Jung, H. S., Lee, E. J., Kim, T. K., Kim, T. N., et al. (2016). Ginsenoside Rg3 prevents INS-1 cell death from intermittent high glucose stress. *Islets* 8 (3), 57–64. doi:10.1080/19382014.2016.1161874
- Langfelder, P., and Horvath, S. (2008). WGCNA: an R package for weighted correlation network analysis. *BMC Bioinf.* 9 (1), 559. doi:10.1186/1471-2105-9-559
- Langfelder, P., Luo, R., Oldham, M. C., and Horvath, S. (2011). Is my network module preserved and reproducible? *PLoS Comput. Biol.* 7 (1), e1001057. doi:10.1371/journal.pcbi.1001057
- Langmead, B., and Salzberg, S. L. (2012). Fast gapped-read alignment with Bowtie 2. *Nat. Methods* 9 (4), 357–359. doi:10.1038/nmeth.1923
- Leung, K. W., and Wong, A. S. (2010). Pharmacology of ginsenosides: a literature review. *Chin. Med.* 5 (20), 20–27. doi:10.1186/1749-8546-5-20
- Li, H., Handsaker, B., Wysoker, A., Fennell, T., Ruan, J., Homer, N., et al. (2009). The sequence alignment/map format and SAMtools. *Bioinformatics* 25 (16), 2078–2079. doi:10.1093/bioinformatics/btp352
- Love, M. I., Huber, W., and Anders, S. (2014). Moderated estimation of fold change and dispersion for RNA-seq data with DESeq2. *Genome Biol.* 15 (12), 550. doi:10.1186/s13059-014-0550-8
- Lu, L., Sun, X., Chen, C., Qin, Y., and Guo, X. (2018). Shexiang baixin pill, derived from the traditional Chinese medicine, provides protective roles against cardiovascular diseases. *Front. Pharmacol.* 9, 1161. doi:10.3389/fphar.2018.01161
- Mitsos, S., Katsanos, K., Koletsis, E., Kagadis, G. C., Anastasiou, N., Diamantopoulos, A., et al. (2012). Therapeutic angiogenesis for myocardial ischemia revisited: basic biological concepts and focus on latest clinical trials. *Angiogenesis* 15, 1–22. doi:10.1007/s10456-011-9240-2
- Mochizuki, M., Yoo, Y. C., Matsuzawa, K., Sato, K., Saiki, I., Tono-oka, S., et al. (1995). Inhibitory effect of tumor metastasis in mice by saponins, ginsenoside-Rb2, 20(R)- and 20(S)-ginsenoside-Rg3, of red ginseng. *Biol. Pharm. Bull.* 18 (9), 1197–1202. doi:10.1248/cpb.37.322910.1248/bpb.18.1197
- Mohamad Zobir, S. Z., Choi, R. J., Modos, D., Fan, T.-P., and Bender, A. (Forthcoming submitted). Predicting and understanding synergistic pairwise compound combinations of Shexian Baixin Pill (SBP) using network biology. *Synergy*, 10073–169. doi:10.1016/j.synres.2021.100073
- Morisaki, N., Watanabe, S., Tezuka, M., Zenibayashi, M., Shiina, R., Koyama, N., et al. (1995). Mechanism of angiogenic effects of saponin from Ginseng Radix rubra in human umbilical vein endothelial cells. *Br. J. Pharmacol.* 115 (7), 1188–1193. doi:10.1111/j.1476-5381.1995.tb15023.x
- Muñoz-Chápoli, R., Quesada, A. R., and Angel Medina, M. (2004). Angiogenesis and signal transduction in endothelial cells. *Cell. Mol. Life Sci.* 61 (17), 2224–2243. doi:10.1007/s00018-004-4070-7
- Orhan, G., Bayram, A., Zer, Y., and Balci, I. (2005). Synergy tests by E test and checkerboard methods of antimicrobial combinations against *Brucella melitensis*. *J. Clin. Microbiol.* 43 (1), 140–143. doi:10.1128/JCM.43.1.140-143.2005
- Pagès, H., Carlson, M., Falcon, S., and Li, N. (2018). *AnnotationDbi: annotation database interface. R package version 1.44.0(AnnotationDbi)*.
- R Core Team (2018). *A language and environment for statistical computing*. Vienna, Austria: R Foundation for Statistical Computing.
- R Development Core Team (2010). *RStudio: integrated development environment for R. 551 ed., 0.97*. Boston, MA: Rstudio.
- Schaefer, C. F., Anthony, K., Krupa, S., Buchoff, J., Day, M., Hannay, T., et al. (2009). PID: the pathway interaction database. *Nucleic Acids Res.* 37 (Database issue), D674–D679. doi:10.1093/nar/gkn653
- Seumois, G., Zapardiel-Gonzalo, J., White, B., Singh, D., Schulten, V., Dillon, M., et al. (2016). Transcriptional profiling of Th2 cells identifies pathogenic features associated with asthma. *J. Immunol.* 197 (2), 655–664. doi:10.4049/jimmunol.1600397
- Shen, W., Fan, W. H., and Shi, H. M. (2010). Effects of shexiang baixin pill on angiogenesis in atherosclerosis plaque and ischemic myocardium. *Zhongguo Zhong Xi Yi Jie He Za Zhi* 30 (12), 1284–1287.
- Sottile, J. (2004). Regulation of angiogenesis by extracellular matrix. *Biochim. Biophys. Acta.* 1654 (1), 13–22. doi:10.1016/j.bbcan.2003.07.002
- Staton, C. A., Stribbling, S. M., Tazzyman, S., Hughes, R., Brown, N. J., and Lewis, C. E. (2004). Current methods for assaying angiogenesis *in vitro* and *in vivo*. *Int. J. Exp. Pathol.* 85 (5), 233–248. doi:10.1111/j.0959-9673.2004.00396.x
- Subramanian, A., Tamayo, P., Mootha, V. K., Mukherjee, S., Ebert, B. L., Gillette, M. A., et al. (2005). Gene set enrichment analysis: a knowledge-based approach for interpreting genome-wide expression profiles. *Proc. Natl. Acad. Sci. U.S.A.* 102 (43), 15545–15550. doi:10.1073/pnas.0506580102
- Sun, C., Yu, Y., Wang, L., Wu, B., Xia, L., Feng, F., et al. (2016). Additive antiangiogenesis effect of ginsenoside Rg3 with low-dose metronomic temozolomide on rat glioma cells both *in vivo* and *in vitro*. *J. Exp. Clin. Oncol.* 35, 32. doi:10.1186/s13046-015-0274-y
- Sun, M., Ye, Y., Xiao, L., Duan, X., Zhang, Y., and Zhang, H. (2017). Anticancer effects of ginsenoside Rg3 (review). *Int. J. Mol. Med.* 39 (3), 507–518. doi:10.3892/ijmm.2017.2857
- Vlot, A. H. C., Aniceto, N., Menden, M. P., Ulrich-Merzenich, G., and Bender, A. (2019). Applying drug synergy metrics to oncology combination screening data: agreements, disagreements and pitfalls. *Drug Discov. Today* 24, 2286. doi:10.1016/j.drudis.2019.09.002
- Working Group on the Summit on Combination Therapy for CVD Yusuf, S., Attaran, A., Bosch, J., Joseph, P., Lonn, E., et al. (2014). Combination pharmacotherapy to prevent cardiovascular disease: present status and challenges. *Eur. Heart J.* 35 (6), 353–364. doi:10.1093/eurheartj/ehu407
- Wu, F., Song, H., Zhang, Y., Zhang, Y., Mu, Q., Jiang, M., et al. (2015). Irisin induces angiogenesis in human umbilical vein endothelial cells *in vitro* and in zebrafish embryos *in vivo* via activation of the ERK signaling pathway. *PLoS One* 10 (8), e0134662. doi:10.1371/journal.pone.0134662
- Wu, G., Chen, L., Gu, Y., Hong, Y., Ma, J., Zheng, N., et al. (2020). Exploring the mechanism underlying the cardioprotective effect of shexiang baixin pill on acute myocardial infarction rats by comprehensive metabolomics. *J. Ethnopharmacol.* 259, 113001. doi:10.1016/j.jep.2020.113001
- Wu, J. X., Liang, C., and Ren, Y. S. (2009). Effects of shexiang baixin pill on function and nitric oxide secretion of endothelial progenitor cells. *Zhongguo Zhong Xi Yi Jie He Za Zhi* 29 (6), 511–513.
- Xiang, L., Jiang, P., Wang, S., Hu, Y., Liu, X., Yue, R., et al. (2013). Metabolomic strategy for studying the intervention and the synergistic effects of the shexiang baixin pill for treating myocardial infarction in rats. *Evid. Based Complement. Alternat. Med.* 2013, 823121–823211. doi:10.1155/2013/823121
- Xiang, L., Jiang, P., Zhan, C., Chen, Z., Liu, X., Huang, X., et al. (2012). The serum metabolomic study of intervention effects of the traditional Chinese medicine Shexiang Baixin Pill and a multi-component medicine poly pill in the treatment of myocardial infarction in rats. *Mol. Biosyst.* 8 (9), 2434–2442. doi:10.1039/C2MB25172H
- Yan, S. K., Zhang, W. D., Liu, R. H., and Zhan, Y. C. (2006). Chemical fingerprinting of Shexiang Baixin Pill and simultaneous determination of its major constituents by HPLC with evaporative light scattering detection and electrospray mass spectrometric detection. *Chem. Pharm. Bull.* 54 (7), 1058–1062. doi:10.1248/cpb.54.1058
- Yan, S., Yang, Y., Wu, Y., Liu, R., and Zhang, W. (2009). Chemical fingerprinting and quantitative analysis of volatiles in Shexiang Baixin Pill by gas chromatography with flame ionization and mass spectrometric detection. *J. Anal. Chem.* 64 (2), 149–155. doi:10.1134/S1061934809020105
- Yilmaz, A., Kliche, S., Mayr-Beyrle, U., Fellbrich, G., and Waltenberger, J. (2003). P38 MAPK inhibition is critically involved in VEGFR-2-mediated endothelial cell survival. *Biochem. Biophys. Res. Commun.* 306 (3), 730–736. doi:10.1016/S0006-291X(03)01064-7
- Zhang, K. J., Zhu, J. Z., Bao, X. Y., Zheng, Q., Zheng, G. Q., and Wang, Y. (2017). Shexiang baixin pills for coronary heart disease in animal models: preclinical evidence and promoting angiogenesis mechanism. *Front. Pharmacol.* 8, 404. doi:10.3389/fphar.2017.00404
- Zhou, W., Chai, H., Lin, P. H., Lumsden, A. B., Yao, Q., and Chen, C. (2005). Ginsenoside Rb1 blocks homocysteine-induced endothelial dysfunction in porcine coronary arteries. *J. Vasc. Surg.* 41 (5), 861–868. doi:10.1016/j.jvs.2005.01.054
- Zobir, S. Z. M., Choi, R. J., Modos, D., Fan, T.-P., and Bender, A. (Forthcoming submitted). Predicting and understanding synergistic pairwise compound combinations of Shexian Baixin Pill (SBP) using network biology. *Synergy*, 100073. doi:10.1016/j.synres.2021.100073

Conflict of Interest: The authors declare that the research was conducted in the absence of any commercial or financial relationships that could be construed as a potential conflict of interest.

Copyright © 2021 Choi, Mohamad Zobir, Alexander-Dann, Sharma, Ma, Lam, Yeo, Zhang, Fan and Bender. This is an open-access article distributed under the terms of the Creative Commons Attribution License (CC BY). The use, distribution or reproduction in other forums is permitted, provided the original author(s) and the copyright owner(s) are credited and that the original publication in this journal is cited, in accordance with accepted academic practice. No use, distribution or reproduction is permitted which does not comply with these terms.